



## Preparation of a novel chelating resin containing amidoxime–guanidine group and its recovery properties for silver ions in aqueous solution

Yang Wang, Xiaojie Ma, Yanfeng Li<sup>\*</sup>, Xiaoli Li, Liuqing Yang, Lei Ji, Yin He

State Key Laboratory of Applied Organic Chemistry, Key Laboratory of Nonferrous Metal Chemistry and Resources Utilization of Gansu Province, College of Chemistry and Chemical Engineering, College of Resources and Environment, Institute of Biochemical Engineering & Environmental Technology, Lanzhou University, Lanzhou 730000, PR China

### HIGHLIGHTS

- ▶ The resin containing amidoxime–guanidine functional group was firstly synthesized.
- ▶ All synthesized processes were done at moderate conditions.
- ▶ The resulting adsorbent has excellent adsorption for Ag(I) in aqueous solution.
- ▶ Removal percentage for Ag(I) could reach almost 100% at low concentration.
- ▶ The resin shows excellent selectivity separate for Ag(I) and can be easily desorbed.

### ARTICLE INFO

#### Article history:

Received 15 May 2012

Received in revised form 31 July 2012

Accepted 31 July 2012

Available online 9 August 2012

#### Keywords:

Amidoxime–guanidine

Chelating resin

Selective adsorption

Desorption

Silver recovery

### ABSTRACT

A novel chelating resin containing amidoxime–guanidine functional group, PSGA resin, has been first synthesized from the functionalization of chloromethylated poly (styrene–divinylbenzene) (CMPS) bead with dicyandiamide (DCDA); the nitrile group in MPS/DCDA bead was changed into amidoxime group by treatment with hydroxylamine under alkaline condition, successively. The resulting PSGA resin was characterized with the Fourier transform infrared spectra (FT-IR), scanning electron microscopy (SEM), elemental analysis and Brunauer–Emmett–Teller (BET). Meanwhile, the adsorption behavior of the PSGA resin for Ag(I) in aqueous solution was investigated by batch method. It is noteworthy that, the adsorption of the resulting PSGA resin for Ag(I) could reach almost 100% in a wide range of pH when an initial concentration of Ag(I) was below 400 mg L<sup>-1</sup>. Furthermore, the PSGA resin can selectively separate Ag(I) in the case of coexisting Zn(II), Cd(II), Mg(II) and Ni(II), and Ag(I) adsorbed by PSGA resin could be easily desorbed.

© 2012 Elsevier B.V. All rights reserved.

### 1. Introduction

As a noble metal, silver is extensively used in various industrial aspects, such as photographic, electroplating, imaging industry, chemical engineering, medication, and coinage and jewellery industries [1]. With the development of all these industries, more and more water pollution containing silver ions is discharged into environment. Compared with the wide applications, silver resources have become relatively short. Simultaneously, silver ions can be accumulated in organisms (including humans) through chains and have caused numerous diseases and disorders [2–4]. For this reason, recovering and removing the Ag(I) from waste water prove to be a knotty problem. Traditional methods to remove the Ag<sup>+</sup> from its effluents include chemical precipitation [5], ion-exchange [6], ultrafiltration [7] and adsorption [8–10], etc. Above

all methods, adsorption is considered to be one of the most efficacious and economical progress since the adsorption materials can be easily synthesized and be environment friendly. Chelating resins, using adsorption method, are intensively focused because of their strong adsorption capacity and high selectivity [11].

Chelating resins often contain amino, carboxy, oxo, thio, phosphoryl as their chelating ligands, N, O, S and P acting their donor atoms [12]. According to the Hard–Soft Acid Base (HSAB) theory by Pearson [13], silver ions show a strong affinity to the ligands including N atoms because that silver ion is a soft Lewis acid and has smaller effective ionic radii [14]. Consequently, we could imagine that the chelating ligands having more N atoms may be adopted by silver ions. Many chelating ligands containing N atoms are used for the adsorption and separation of silver ions, amidoxime group is commonly reported among them. With its extraordinary metal ions adsorption performance and mature synthesis, amidoxime is widely used in lots of industries especially in wastewater containing heavy metal handling [15].

<sup>\*</sup> Corresponding author. Fax: +86 931 8912113.

E-mail address: [liyf@lzu.edu.cn](mailto:liyf@lzu.edu.cn) (Y. Li).

Since most articles synthesized amidoxime group are involved in the conversion of a nitrile group into an amidoxime, none of them is used the nitrile of the cyanoguanidine. After the conversion of the nitrile of the cyanoguanidine into amidoxime, the chelating group has more efficient metal coordination sites, and the excellent adsorption behavior of the resin for metal ions is extremely worth to be expected. However, the relevant work has rarely been reported up to now. In view of this, we use the cyanoguanidine reacting with hydroxylamine hydrochloride to introduce the amidoxime group and synthesize the amidoxime guanidine group [16]. Amidoxime guanidine with a unique molecular structure which owes as many as five N atoms in one molecular can be supposed having the strong adsorption capacity for silver ions.

The ultimate goal of this study is to synthesis a novel chelating resin contain amidoxime guanidine group which be hoped to have a strong affinity to silver ions. In this work, we prepared the chelating resin with the simple method that modified CMPS with two steps in aqueous phase without any other toxic organic agent except materials. The FT-IR, SEM, elemental analysis and BET was used to characterize the resulted PSGA resin. The obtained resin shows excellent adsorption capacity and high selectively for silver ions decided by batch and column methods, regeneration of the resins was also studied to estimate the capacity in silver ions removing and recovering industries.

## 2. Experiment

### 2.1. Materials

CMPS beads holding 7% of crosslinking degree, 18.92% of chloride content and 14.3 nm of average pore radius were purchased from Xi'an (China). Dicyandiamide, hydroxylamine hydrochloride, tetrabutylammonium bromide and all other reagents with analytical reagent grade were commercially obtained and used as received.  $\text{AgNO}_3$ ,  $\text{Zn}(\text{NO}_3)_2 \cdot 6\text{H}_2\text{O}$ ,  $\text{Cd}(\text{NO}_3)_2 \cdot 4\text{H}_2\text{O}$ ,  $\text{Mg}(\text{NO}_3)_2 \cdot 6\text{H}_2\text{O}$ ,  $\text{Ni}(\text{NO}_3)_2$  were used as sources for Ag(I), Zn(II), Cd(II), Ni(II) and Mg(II), respectively.

### 2.2. Apparatus

The FT-IR was recorded with a Nicolet Magna-IR 550 spectrophotometer between 4000 and  $450\text{ cm}^{-1}$  using the KBr pellet technique. The shapes and morphology of the resins were observed by JSM-6701F scanning electron microscope, JEOL, Japan, operating at 5.0 kV. The pore volume, pore diameter, and BET surface area were determined by a Quantachrome NovaWin2 Instrument. Elemental analysis performed by a PerkinElmer 2400 CHN analyzer. The concentration of ions in solution was determined by an inductively coupled plasma spectrometer (ICP/IRIS Advantage, Thermo, America).

### 2.3. Preparation of PS-DCDA resin

PS-DCDA was prepared according to our previously published procedure [17]. 10 g CMPS was swollen in DMF for 8 h in a 250 mL three-necked glass flask with mechanical stirrer. A solution of 12.5 mL DMF containing 18.5 g dicyandiamide and 2 g phase transfer catalyst of tetrabutylammonium bromide was added in the flask. Then the mixture was stirred at room temperature and 12 mL KOH solution (50%) was dropped in the system within an hour. Afterwards, the reaction temperature was raised to  $55\text{ }^\circ\text{C}$  gradually with continuous stirring for 12 h. The prepared samples were washed several times by hot water to remove residual dicyandiamide, rinsed thoroughly with distilled water and dried at  $60\text{ }^\circ\text{C}$  for 24 h in vacuum to obtain the PS-DCDA.

### 2.4. Preparation of PSGA

Twenty-one gram hydroxylamine hydrochloride dissolved in 150 mL methanol solution (methanol: water/5:1), about 11.9 g NaOH dissolved in 50 mL water was added in the above methanol solution to neutralize the HCl. Then NaCl generated from the neutralization reaction was filtered out and the pH of hydroxylamine solution was adjusted to 10 by adding NaOH solution as standby. In reference to the reported work [17], the concrete amidoximation process was as follows: maintaining the reaction medium as methanol to water ratio 5:1, about 10 g produced PS-DCDA resin and above prepared hydroxylamine solution was added in the three-necked glass flask fitted with reflux condenser and mechanical stirrer. Then the reaction was controlled at  $70\text{ }^\circ\text{C}$  with continuous stirring for 4 h. Finally, the prepared sample was collected using filter, washed with distilled water and was dried at  $60\text{ }^\circ\text{C}$  for 24 h under vacuum. The product obtained was abbreviated to be PSGA in this paper. The synthesis routine of the resin was shown in Fig. 1.

### 2.5. Adsorption experiment using batch methods

The adsorption of silver ions was studied for batch experiments which were carried out by placing 0.1 g resin in series of flasks containing ions aqueous solution (50 mL) with the desired initial concentration and pH. Then the flasks were shaken in a thermostat oscillator under dark environment with constant rate 130 rpm at specific temperature for a given time.

To investigate the effect of pH, we carefully adjusted the initial pH of ions aqueous solution between 2.0 and 6.0 by adding a certain amount of  $\text{HNO}_3$  or NaOH solutions with different pH values. The working concentration of silver ions was used in the range of  $300\text{--}600\text{ mg L}^{-1}$  for kinetic studies and  $150\text{--}400\text{ mg L}^{-1}$  for isotherm studies. The selective separation of Ag(I) from mixtures with Ni(II), Zn(II), Cd(II), Mg(II) was carried at all ions concentration  $200\text{ mg L}^{-1}$ . The residual concentration of metal ions was measured by ICP. The amount of silver ions adsorbed per gram of the resin was calculated on the basis of following equation.

$$Q_e = \frac{(C_0 - C_e)V}{M} \quad (1)$$

$$\text{Adsorption efficient} = \frac{C_0 - C_e}{C_0} \times 100\% \quad (2)$$

where  $Q_e$  is the adsorption capacity ( $\text{mg g}^{-1}$ );  $C_0$  and  $C_e$  are initial and equilibrium concentrations of the Ag(I) ( $\text{mg L}^{-1}$ ) in the testing solution ( $\text{mg L}^{-1}$ );  $V$  is the volume of the solution (L), and  $M$  is the weight of resin beads (g).

### 2.6. Column experiments

Column experiments were performed in a glass column ( $27\text{ cm} \times 7\text{ cm}$ ) with a small piece of glass wool at the bottom. One gram of resin was introduced into the column, and Ag(I) solution with initial concentration  $200\text{ mg g}^{-1}$  was flowed downward through the column at flow rate of  $0.5\text{ mL min}^{-1}$ . Samples were collected at different time intervals and analyzed for Ag(I) concentration by spectrophotometric method.

### 2.7. Desorption and regeneration experiments

Desorption experiments were carried out by placing 0.1 g PSGA resin which getting saturated sorption in  $400\text{ mg g}^{-1}$  Ag(I) solution in series of flasks containing 50 mL different eluents and shaking at  $30\text{ }^\circ\text{C}$  for 4 h. Chose the best eluent determined by recovery capacity and repeated above processes for six time to estimate the regeneration performance.

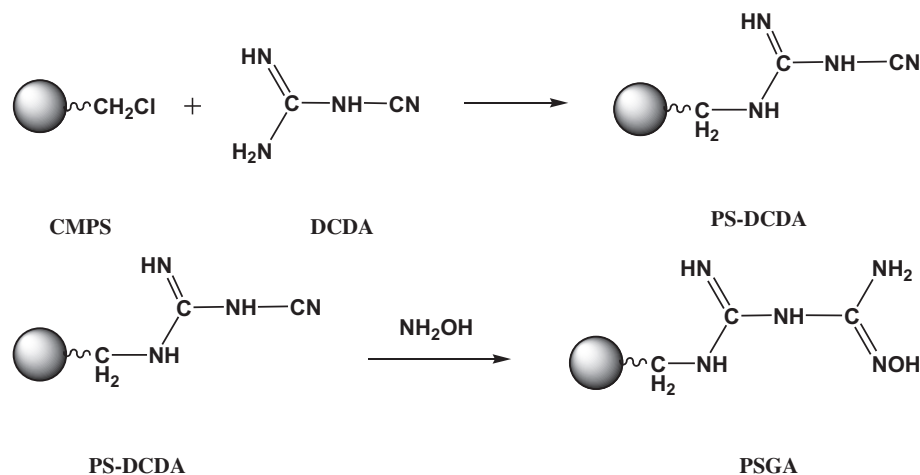


Fig. 1. Scheme for the synthesis route of PS-DCDA and PSGA.

### 3. Results and discussion

#### 3.1. Characteristic of resins

The CMPS, synthesized PS-DCDA and PSGA resins were characterized by FI-IR and their spectra are given in Fig. 2. By compared of CMPS and PS-DCDA, the adsorption band around  $670\text{ cm}^{-1}$  and  $1262\text{ cm}^{-1}$  revealed the stretching vibration of  $\text{CH}_2\text{-Cl}$  group in CMPS disappeared in the curve of PS-DCDA, and the new bands near  $2174\text{ cm}^{-1}$  and  $1568\text{ cm}^{-1}$  corresponding to  $\nu_{\text{C}\equiv\text{N}}$  and  $\nu_{\text{N}-\text{C}\equiv\text{N}}$ , respectively, characterized the PS-DCDA as expected. After amidoxime preparation, the CN band of  $2174\text{ cm}^{-1}$  almost disappeared and the new bond of amidoxime at  $1621\text{ cm}^{-1}$  was formed [18]. These observations reveal that the studied resin was successfully synthesized with harmless and low-cost raw materials.

Fig. 3 shows the shape and surface morphologies of beads which are studied by SEM. It can be seen from Fig. 3a that CMPS bead exhibits as a perfect ball, and the macroporous structure uniformly distributed on the surface of CMPS are visible (Fig. 3b). In addition, compared to the surface of CMPS, it is found that the macroporous structure on PSGA still exists, and the pore space on the surface of PSGA slightly increased because of the introduction of chelating group to CMPS. Moreover, it is interesting to observe that many crystals evenly distributed on the surface of

the PSGA after the silver ions were adsorbed (Fig. 3d). We inferred that the substance on the PSGA was silver deposition, resulting from the instability of silver ions and the reduction properties of some organic groups. As reported, heavy metal ions like  $\text{Ag}^+$  with a high standard reduction potential, can be reduced to metals by some functional groups like  $-\text{NH}_2$ ,  $-\text{CN}$ , etc. [19–22]. It is also observed that the silver deposition is extremely unstable, which could be easily oxidized to black silver oxide in a certain time [23–25].

The pore volume, pore diameter, and BET area of the CMPS and PSGA resins were given in Table 1. We could find that the pore volume, pore diameter and BET surface area of PS-DCDA drastic increased compared with CMPS due to the guanidine groups grafted on CMPS. And the proportion of N, C, H in CMPS, PS-DCDA and PSGA resins performed by elemental analysis were also listed in Table 2.

#### 3.2. The effect of pH on Ag(I) adsorption

Fig. 4 shows the effect of acidity of solution on the adsorption of Ag(I) which was discussed in range of pH 2–6. We can see that the adsorption of PS-DCDA for Ag(I) is pH dependent, and it is better to keep the operating pH at 3–5 due to the great availability of free amino groups [17]. A strong acidic environment would make Ag(I) compete with  $\text{H}_3\text{O}^+$  for an active site, resulting in the decrease of Ag(I) adsorption amount. However, the adsorption ability of PSGA for Ag(I) were not affected very much by the pH values, and it is noted that after the introduction of amidoxime group ( $-\text{C}(\text{NH}_2)=\text{N}-\text{OH}$ ), the adsorption capacity of PSGA for Ag(I) enhances greatly by comparing with PS-DCDA. Results indicated that the extended functional groups enhanced the competitive ability of PSGA for Ag(I).

#### 3.3. The effect of contacting time on Ag(I) adsorption

The relationship between adsorption amount and contact time was displayed in Fig. 5. As presented in Fig. 5, all the adsorption capacity with different initial concentration increased with prolonging of reaction time, and the adsorption of Ag(I) on PSGA was very rapid with an increase in contact time from 0 to 100 min resulting from the high concentration of Ag(I) at primary adsorption period. While after 5 h, all the adsorption curves with the three different initial concentration (Fig. 5), became very gentle because of diffusive resistance of Ag(I) on the resin, meaning that the equilibrium have been reached. Furthermore, the result of

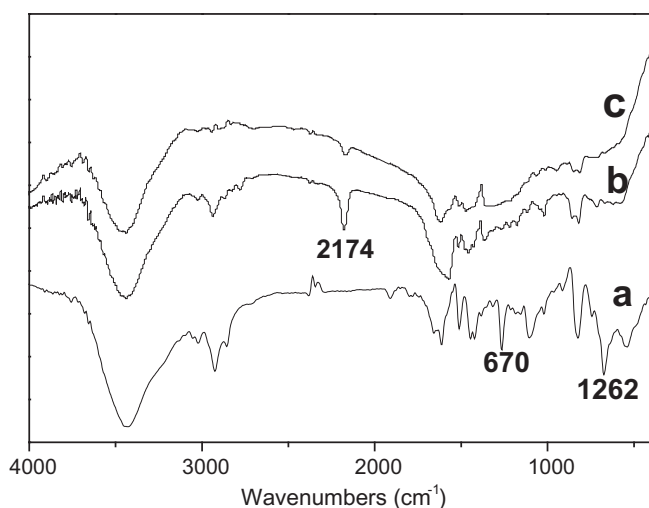


Fig. 2. FI-IR spectrum of CMPS (a); PS-DCDA (b) and PSGA (c).

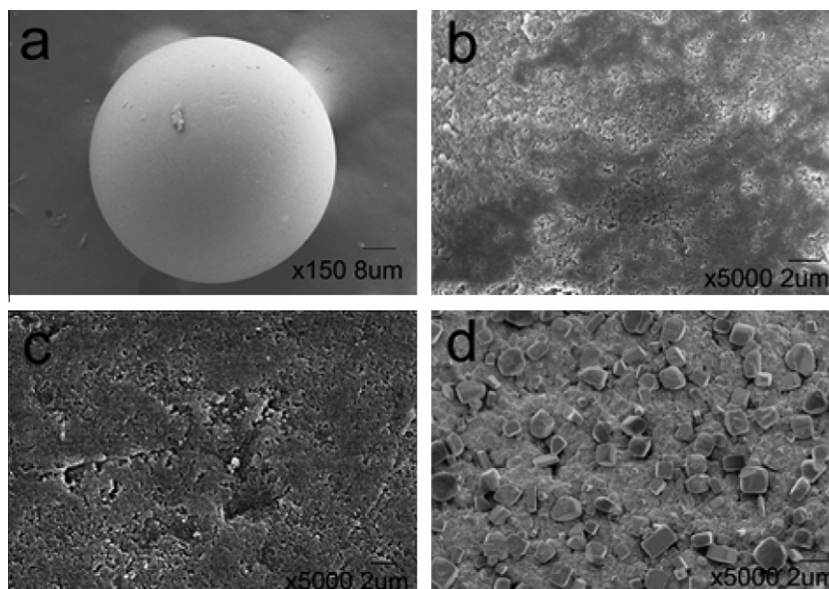


Fig. 3. SEM images of the shape of CMPS (a) and surface morphologies of the beads: CMPS (b), PSGA (c), PSGA after adsorption of Ag(I) (d).

**Table 1**  
The BET surface area of resins.

The resin	BET surface area ( $\text{m}^2 \text{g}^{-1}$ )	Pore volume ( $\text{cm}^3 \text{g}^{-1}$ )	Pore diameter (nm)
CMPS	59.2027	0.309624	21.17328
PSGA	60.8978	0.359043	23.81154

**Table 2**  
Compositions of the resin and related intermediates.

Resin	N%	C%	H%
CMPS	0.00	71.21	5.43
PS-DCDA	7.79	70.13	6.86
PSGA	6.63	61.82	6.79

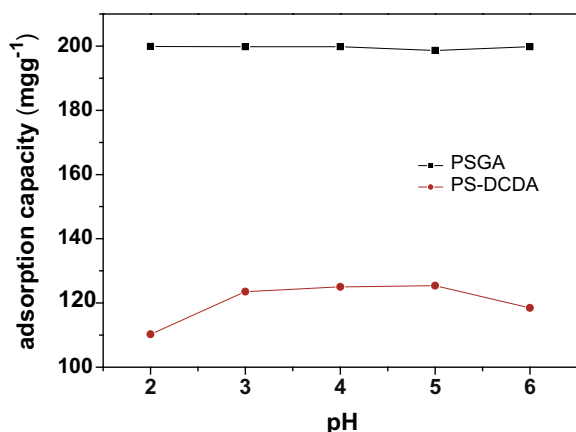


Fig. 4. Effect of initial pH on Ag(I) adsorption by 0.1 g resin with an initial concentration of  $400 \text{ mg L}^{-1}$  at  $30^\circ\text{C}$ .

the experiment suggested the equilibrium time closely related to the initial concentration. Higher initial concentration resulted to higher drive force coming from the concentration variance of between Ag(I) solution and the resin, which favors Ag(I) adsorption. But adsorption at all three different initial concentrations have

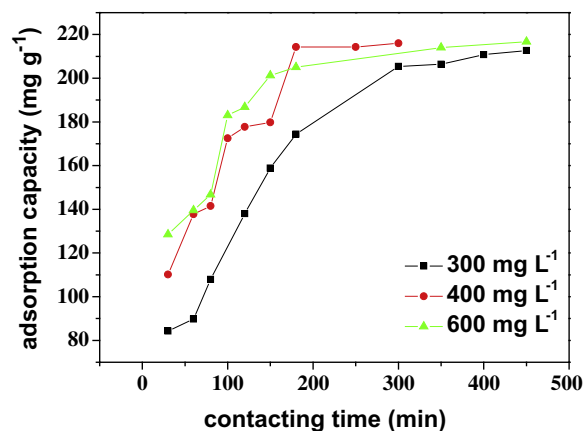


Fig. 5. Effect of shaking time on Ag(I) adsorption with different initial concentration at  $30^\circ\text{C}$ .

almost the same adsorption amount  $210 \text{ mg g}^{-1}$  after equilibrium. Therefore, choosing a proper initial concentration by judging from contact time is very important to the adsorption process.

### 3.4. Effect of initial concentration

Fig. 6 shows the effect of initial concentration on the adsorption of Ag(I), through chart analysis, we surprised to find that when the adsorption capacity value was less than  $210 \text{ mg g}^{-1}$ , the adsorption capacity at equilibrium time increased rapidly with initial concentration and the removal percentage of Ag(I) almost reaching 100%, but when the adsorption capacity value is more than  $210 \text{ mg g}^{-1}$ , the initial concentration has little effect on adsorption capacity. This could be easily explained by the SEM image (Fig. 3d), the pores of the resin was completely stuffed by  $\text{Ag}_2\text{O}$  crystals when the resins reaching saturated adsorption, which prevented the further adsorption of silver ions. Therefore, as Fig. 6 showed, when the initial concentration is below  $400 \text{ mg g}^{-1}$ , the resins could nearly adsorb all the silver ions in solutions, but could only achieve the saturation adsorption if the concentration is above  $400 \text{ mg g}^{-1}$ . The curves of adsorption efficient in Fig. 5 also demonstrated this.

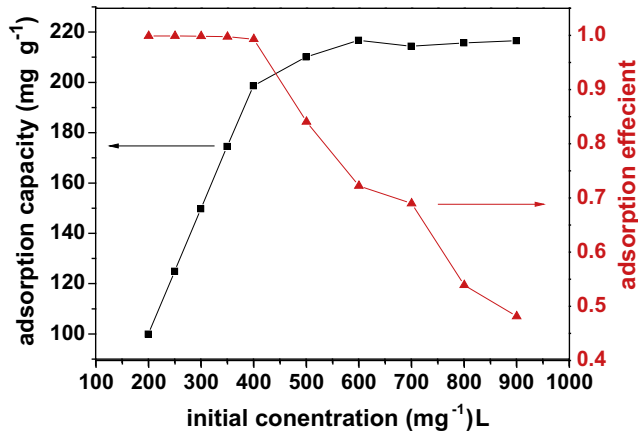


Fig. 6. Effect of initial concentration on Ag(I) adsorption at 30 °C.

### 3.5. Adsorption kinetics

We elucidated the reaction kinetic parameters for the adsorption process by the pseudo-first-order, pseudo-second-order and intraparticle diffusion kinetic models in this work [26–28].

The pseudo-first-order (2), pseudo-second-order (3) and intraparticle diffusion (4) kinetic model are respectively represented as:

$$\log(Q_e - Q_t) = \log Q_e - \frac{k_1 t}{2.303} \quad (3)$$

$$\frac{t}{Q_t} = \frac{1}{k_2 Q_e^2} + \frac{t}{Q_e} \quad (4)$$

$$Q_t = k_i t^{1/2} + C \quad (5)$$

where  $k_1$ ,  $k_2$  and  $k_i$  are pseudo-first-order rate constant ( $\text{min}^{-1}$ ), pseudo-second-order rate constant ( $\text{g mg}^{-1} \text{min}^{-1}$ ) and intraparticle diffusion rate constant ( $\text{mg g}^{-1} \text{min}^{-1/2}$ ) of adsorption, respectively.  $Q_e$  and  $Q_t$  are the adsorption capacity ( $\text{mg g}^{-1}$ ) at equilibrium time and at time  $t$  (min), respectively.  $C$  ( $\text{mg g}^{-1}$ ) is a constant of intra-particle diffusion model.

The parameters and correlation coefficients ( $R$ ) of the three different models were all showed in Table 3. Compared with other two models, the correlation coefficient of pseudo-second-order kinetics model is much higher obviously. Simultaneously, the calculated  $Q_e$  value of pseudo-second-order kinetic model is more in agreement with experimental  $Q_e$  value than the Lagergren kinetics. Therefore, the pseudo-second-order kinetic model could fit the adsorption of Ag(I) on resins very well, which was based on the assumption that the determining rate step may be chemisorption promoted by covalent forces through the electron exchange, or valency forces through electrons sharing between sorbent and sorbate, indicating that the adsorption of Ag(I) on PSGA is mainly the chemical reactive adsorption.

Table 3  
Parameters of kinetics model for adsorption of Ag(I) on PSGA with different initial concentration.

Initial Conc. (mg L <sup>-1</sup> )	$Q_{\text{exp}}$ (mg g <sup>-1</sup> )	Pseudo-first-order			Pseudo-second-order			Intraparticle diffusion	
		$k_1 \times 10^3$ (min <sup>-1</sup> )	$Q_e$ (mg g <sup>-1</sup> )	$R^a$	$k_2 \times 10^4$ (g g <sup>-1</sup> min <sup>-1</sup> )	$Q_e$ (mg g <sup>-1</sup> )	$R^a$	$K_i$ (mg g <sup>-1</sup> min <sup>-1/2</sup> )	$R^a$
300	212.63	2.17	253.05	0.9785	5.153	181.82	0.9996	0.10	0.9481
400	216.00	4.00	318.35	0.8221	0.7757	256.41	0.9883	0.10	0.913
600	216.68	2.17	24.40	0.955	1.361	232.56	0.9968	0.13	0.7747

### 3.6. Adsorption isotherm

To investigate the adsorption of Ag(I), we selected the data which the resin did not reach the saturated adsorption in Fig. 6 and treated them with Langmuir and Freundlich equations [29,30], respectively.

$$\frac{C_e}{Q_e} = \frac{1}{bQ_{\text{max}}} + \frac{C_e}{Q_{\text{max}}} \quad (6)$$

$$\ln Q_e = \ln K_F + \left(\frac{1}{n}\right) \ln C_e \quad (7)$$

where  $C_e$  is the equilibrium concentration of metal ions in solution ( $\text{mg L}^{-1}$ ), and  $Q_e$  is the equilibrium adsorption capacity ( $\text{mg g}^{-1}$ ),  $Q_{\text{max}}$  ( $\text{mg g}^{-1}$ ) and  $b$  ( $\text{L mg}^{-1}$ ) are the Langmuir constant which are related to the adsorption capacity and energy of adsorption, respectively.  $K_F$  is the Freundlich constant related to adsorption capacity.

The parameters and correlation coefficients ( $R$ ) of Langmuir and Freundlich model were all showed in Table 4. We could clearly see from the correlation coefficients ( $R$ ) that the Langmuir model was found to describe the experiment data more precisely than the Freundlich model at the studied temperature with no doubt. The Langmuir theory was based on an assumption that uptake of metal ions occurs on a homogenous surface by monolayer adsorption without any interaction between adsorbed ions. The  $Q_{\text{max}}$  calculated by Langmuir model was  $212 \text{ mg g}^{-1}$ , exactly consistent with the actual saturated adsorption of resin, which also proved the monolayer adsorption was dominated.

Table 5 compares the maximum adsorption capacity of the PSGA resin for Ag(I) with other adsorbents reported in the literature. Although the thiourea-modified chitosan resin shows the largest adsorption capacity, the PSGA resin, synthesized by industrialized CMPS beads, has much more value of industrial applica-

Table 4  
Parameters of isotherm model for adsorption of Ag(I) on PSGA.

Temperature (K)	Langmuir parameters			Freundlich parameters		
	$Q_{\text{max}}$ (mg g <sup>-1</sup> )	$b$ (L mg <sup>-1</sup> )	$R^a$	$K_F$ (mg g <sup>-1</sup> )	$1/n$	$R^a$
303.15	212.76	5.22	0.9999	166.17	0.24	0.9107

Table 5  
Maximum adsorption capacities of adsorption of Ag(I) onto various adsorbents.

Absorbent	Adsorption capacity (mg g <sup>-1</sup> )
Surface molecular-imprinted biosorbent [31]	199.3
Chemically modified melamine resins [32]	102.6
Chemically modified chitosan with magnetic [33]	226.8
Thiourea-modified chitosan resin [34]	407
PSGA resin (this work)	212



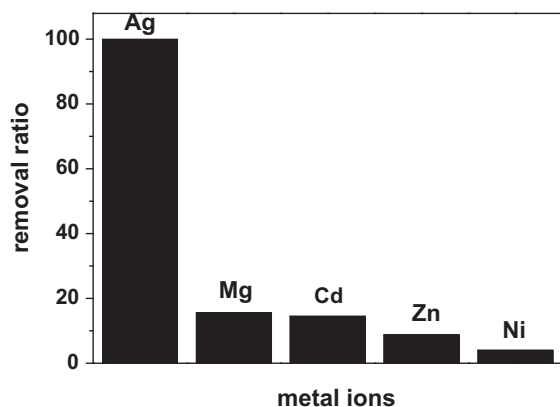


Fig. 7. Effect of some foreign ions on silver adsorption capacity.

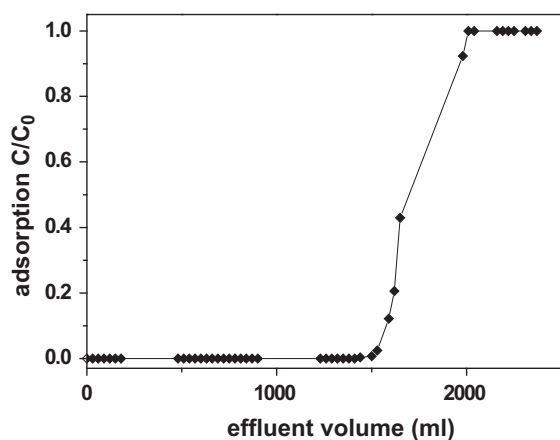


Fig. 8. The breakthrough curve of the PSGA resin.

tions as cost-effective absorbent because of its common industrialized raw materials and mature synthetic routes.

### 3.7. Column adsorption

Column adsorption tests for the adsorption resins have more meaningful in practical application than the batch experiments. Therefore, we allowed Ag(I) solution with initial concentration  $200 \text{ mg L}^{-1}$  to pass through the column packed with the PSGA resin at  $0.5 \text{ mL min}^{-1}$  to research the column adsorption studies. Fig 8 shows the breakthrough curves that were plotted as a dimensionless concentration factor  $C/C_0$  ( $C$ : the concentration of Ag(I) in the solution coming out of column and  $C_0$ : is the concentration of Ag(I) in the feed solution) versus effluent volume. The breakthrough curve indicated that the saturation point was achieved when 2000 mL of Ag(I) solution was used.

### 3.8. Metal ions co-adsorption

The adsorption selectivity is an indispensable factor to evaluate the adsorption properties of the resin comprehensively selective separation of Ag(I) from multiple mixtures with Zn(II), Cd(II), Mg(II) and Ni(II) was investigated in this work. The results of the metal ions co-adsorption were presented in Fig. 7, which could be clearly seen that the adsorption capacity for silver ions was prominent larger than other metal ions and the removal percentage of silver ions reaching 99.95%. Therefore, the PSGA resin has distinct high selectivity for silver ions from the mixed metal ions

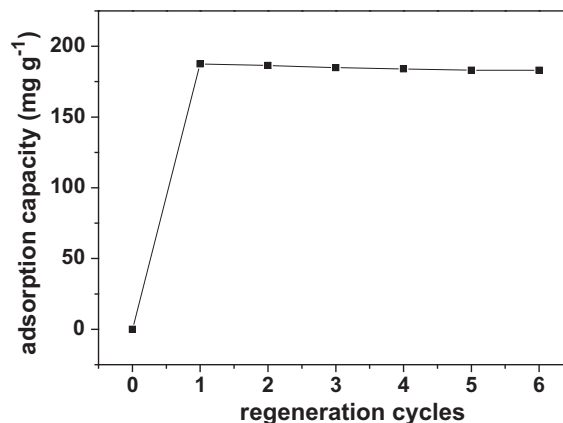


Fig. 9. Adsorption capacity of the PSGA resin after repeated regeneration.

Table 6

Desorption Ag(I) of by different eluents at 30 °C.

Eluent	4 M HCl	6 M HCl	1% Thiourea	3% Thiourea	2MHCl + 1% thiourea
Recovery (%)	58.58	87.72	76.96	81.14	36.55

solution, and can be used to separate silver ions among wastewater with Zn(II), Cd(II), Mg(II) and Ni(II) due to the marked preference to Ag(I).

### 3.9. Desorption and regeneration cycles

The Ag(I) desorption from the resin is necessary in order to reduce the cost of removal process. We used various concentration of thiourea, HCl, and thiourea–HCl, to study desorption efficiency by batch method. The results of different eluents was exhibited in Table 6, which indicated that Ag(I) could be quantitatively desorbed with 50 mL of 6 M HCl with recovery above 87%. Regeneration experiment was carried out using 6 M HCl as the eluent, and the regeneration cycles result was show in Fig 9. It could be found out that the PSGA resin had good regeneration performance and the adsorption capacity decreased little after six time regeneration.

## 4. Conclusions

The chelating resin synthesized through functionalizing the chloromethylated copolymer of styrene-di-vinylbenzene with dicyandiamide, and transforming the nitrile of dicyandiamide into amidoxime in order to obtain the amidoximeguanidine group. It was found out that the PSGA resin had strong adsorption affinity on Ag(I), and the adsorption process was almost unaffected by pH ranging from 2 to 6 and initial metal ion concentration. Simultaneously, the adsorptivity of Ag(I) was over 99% with the initial concentration under  $400 \text{ mg L}^{-1}$  and the resin also has a unique selectivity for Ag(I) from the mixed metal ions solution. The results revealed that the adsorption reaction followed pseudo-second-order kinetic model and fitted well with Langmuir isotherm equation, indicating that chemical adsorption was the rate-control step and the monolayer adsorption was dominated. Synthesized by common industrialized raw materials and mature synthetic routes, having a good adsorption capacity demonstrated by batch and column methods, and also with high selectivity and good reusability on silver ions, the PSGA resin has vary high practical value

in industrial applications as cost-effective absorbent for recovering silver from aqueous solutions or wastewater.

### Acknowledgments

The authors gratefully acknowledge financial supports from the National Major Specific Program of Science and Technology on Controlling and Administering of Water's pollution (2009ZX07212-001-04), the National Natural Science Foundation of China for the scientific research ability training of undergraduate students majoring in chemistry by the two patters based on the tutorial system and top students (J0730425 and J1010067).

### References

- [1] Z. Celik, M. Gülfen, Synthesis of a novel dithiooxamide–formaldehyde resin and its application to the adsorption and separation of silver ions, *J. Hazard. Mater.* 174 (2010) 556–562.
- [2] X.H. Song, P. Gunawan, R.R. Jiang, Surface activated carbon nanospheres for fast adsorption of silver ions from aqueous solutions, *J. Hazard. Mater.* 194 (2011) 162–168.
- [3] M.J. Eckelman, T.E. Graedel, Silver emissions and their environmental impacts: a multilevel assessment, *Environ. Sci. Technol.* 41 (2007) 6283–6289.
- [4] M. Hosoba, K. Oshita, R.K. Katarina, T. Takayanagi, M. Oshima, S. Motomizu, Synthesis of novel chitosan resin possessing histamine moiety and its application to the determination of trace silver by ICP–AES coupled with triplet automated pretreatment system, *Anal. Chim. Acta* 639 (2009) 51–56.
- [5] N. Unlu, M. Ersoz, Adsorption characteristics of heavy metal ions onto a low cost biopolymeric sorbents from aqueous solution, *J. Hazard. Mater.* 136 (2006) 272–280.
- [6] S. Coruh, G. Senel, A comparison of the properties of natural clinoptilolites and their ion-exchange capacities for silver removal, *J. Hazard. Mater.* 180 (2010) 486–492.
- [7] K.P. Desai, Z.V.P. Murthy, Removal of silver from aqueous solutions by complexation–ultrafiltration using anionic polyacrylamide, *Chem. Eng. J.* 185–186 (2012) 187–192.
- [8] X. Lu, Q.F. Yin, Z. Xin, Powerful adsorption of silver(I) onto thiol-functionalized polysilsesquioxane microspheres, *Chem. Eng. Sci.* 65 (2010) 6471–6477.
- [9] M.A. Abd, M.H. Mohamed, K.Z. Elwakeel, Adsorption of silver(I) on synthetic chelating polymer derived from 3-amino-1,2,4-triazole-5-thiol and glutaraldehyde, *Chem. Eng. J.* 151 (2009) 30–38.
- [10] Q.F. Lu, M.R. Huang, X.G. Li, Synthesis and heavy-metal-ion sorption of pure sulfophenylenediamine copolymer nanoparticles with intrinsic conductivity and stability, *Chem. Eur. J.* 13 (2007) 6009–6018.
- [11] A.M. Donia, A.A. Atia, F.I. Abouzayed, Preparation and characterization of nano-magnetic cellulose with fast kinetic properties towards the adsorption of some metal ions, *Chem. Eng. J.* 191 (2012) 22–30.
- [12] M. Tuzen, O.D. Uluozlu, C. Usta, M. Soyak, Biosorption of copper(II), lead(II), iron(III) and cobalt(II) on *Bacillus sphaericus*-loaded Diaion SP-850 resin, *Anal. Chim. Acta* 581 (2007) 241–246.
- [13] G.R. Pearson, Hard and soft acids and bases, *J. Am. Chem. Soc.* 85 (1963) 3533–3539.
- [14] A. Dean, *Lange's Handbook of Chemistry*, fifth ed., McGraw-Hill, Inc., 1999.
- [15] K. Saeed, S. Haider, Preparation of amidoxime-modified polyacrylonitrile (PAN-oxime) nanofibers and their applications to metal ions adsorption, *J. Membr. Sci.* 322 (2008) 400–405.
- [16] A. Nilchi, A.A. Babalou, R. Rafiee, Adsorption properties of amidoxime resins for separation of metal ions from aqueous systems, *React. Funct. Polym.* 68 (2008) 1665–1670.
- [17] X.J. Ma, Y.F. Li, Z.F. Ye, L.Q. Yang, L.C. Zhou, L.Y. Wang, Novel chelating resin with cyanoguanidine group: useful recyclable materials for Hg(II) removal in aqueous environment, *J. Hazard. Mater.* 185 (2011) 1348–1354.
- [18] M.R. Lutfor, Preparation and characterization of poly(amidoxime) chelating resin from polyacrylonitrile grafted sago starch, *Eur. Polym. J.* 36 (2000) 2105–2113.
- [19] S. Majid, M.E. Rhazi, A. Amine, A. Curulli, Carbon paste electrode bulk-modified with the conducting polymer poly(1,8-diaminonaphthalene): application to lead determination, *Microchim. Acta* 143 (2003) 195–205.
- [20] B.J. Pals, M. Skompska, K. Jackowska, Sensitivity of poly 1,8-diaminonaphthalene to heavy metal ions—electrochemical and vibrational spectra studies, *J. Electroanal. Chem.* 433 (1997) 41–48.
- [21] X.G. Li, M.R. Huang, S.X. Li, Facile synthesis of poly(1,8-diaminonaphthalene) microparticles with a very high silver-ion adsorbability by a chemical oxidative polymerization, *Acta Mater.* 52 (2004) 5363–5378.
- [22] X.G. Li, X.L. Ma, J. Sun, Powerful reactive sorption of silver(I) and mercury(II) onto poly(o-phenylenediamine) microparticles, *Langmuir* 25 (2009) 1675–1684.
- [23] M.L. Zheludkevich, A.G. Gusakov, A.G. Voropaev, Oxidation of silver by atomic oxygen, *Oxid. Met.* 61 (2004) 39–48.
- [24] D.B. Oakes, R.H. Krech, B.L. Upschulte, G.E. Caledonia, Oxidation of polycrystalline silver films by hyperthermal oxygen atoms, *J. Appl. Phys.* 77 (1995) 2166–2172.
- [25] M.K. Bhan, P.K. Nag, G.P. Miller, J.C. Gregory, Chemical and morphological changes on silver surfaces produced by microwave generated atomic oxygen, *J. Vac. Sci. Technol. A* 12 (1994) 699–706.
- [26] X.L. Li, Y.F. Li, Z.F. Ye, Preparation of macroporous bead adsorbents based on poly(vinyl alcohol)/chitosan and their adsorption properties for heavy metals from aqueous solution, *Chem. Eng. J.* 178 (2011) 60–68.
- [27] Y.S. Ho, G. McKay, Pseudo-second order model for sorption processes, *Process Biochem.* 34 (1999) 451–465.
- [28] L.Q. Yang, Y.F. Li, H.Y. Hu, X.L. Jin, Z.F. Ye, Preparation of novel spherical PVA/ATP composites with macroreticular structure and their adsorption behavior for methylene blue and lead in aqueous solution, *Chem. Eng. J.* 173 (2011) 446–455.
- [29] G.D. Sheng, S.W. Wang, J. Hu, J.X. Li, X.K. Wang, Adsorption of Pb(II) on diatomite as affected via aqueous solution chemistry and temperature, *Colloids Surf. A* 339 (2009) 159–166.
- [30] S.T. Yang, J.X. Li, X.K. Wang, Sorption of Ni(II) on GMZ bentonite: effects of pH, ionic strength, foreign ions, humic acid and temperature, *Appl. Radiat. Isot.* 67 (2009) 1600–1608.
- [31] H. Huo, H. Su, T. Tan, Adsorption of Ag<sup>+</sup> by a surface molecular-imprinted biosorbent, *Chem. Eng. J.* 150 (2009) 139–144.
- [32] M.A. Abd El-Ghaffar, Z.H. Abdel-Wahab, K.Z. Elwakeel, Extraction and separation studies of silver(I) and copper(II) from their aqueous solution using chemically modified melamine resins, *Hydrometallurgy* 96 (2009) 27–34.
- [33] A.M. Donia, A.A. Atia, K.Z. Elwakeel, Recovery of gold(III) and silver(I) on a chemically modified chitosan with magnetic properties, *Hydrometallurgy* 87 (2007) 197–206.
- [34] L. Wang, R.G. Xing, S. Liu, P.C. Li, Recovery of silver(I) using a thiourea-modified chitosan resin, *J. Hazard. Mater.* 180 (2010) 577–582.